JOURNAL OF MATERIALS SCIENCE **36** (2001) 5203–5211

# A comparative study on copper corrosion originated by formic and acetic acid vapours

A. LÓPEZ-DELGADO, E. CANO, J. M. BASTIDAS, F. A. LÓPEZ
*National Centre for Metallurgical Research (CSIC), Avda. Gregorio del Amo 8, 28040 Madrid, Spain*
*E-mail: bastidas@cenim.csic.es*

The copper corrosion rate and products originated by the action of formic and acetic acid vapours at a 100% relative humidity were studied. Copper specimens were exposed to formic and acetic acid vapours for a period of 21 days. Five formic and acetic acid vapour concentrations (10, 50, 100, 200 and 300 ppm) were tested. Copper corrosion rates of up to 1300 mg $m^{-2}$ $d^{-1}$ (mmd) for formic acid and up to 2300 mmd for acetic acid were measured using a gravimetric method. The corrosion-product layers were characterised using electrochemical, X-ray powder diffraction and scanning electron microscopy techniques. Some of the compounds identified were: cuprite ($Cu_2O$), for both acids; cupric hydroxide monohydrate ($Cu(OH)_2 \cdot H_2O$) and copper formate tetrahydrate ($Cu(HCOO)_2 \cdot 4H_2O$), for formic acid; and copper acetate dihydrate ($Cu(CH_3COO)_2 \cdot 2H_2O$) and copper hydroxide acetate dihydrate ($Cu_4(OH)(CH_3COO)_7 \cdot 2H_2O$), for acetic acid.
© *2001 Kluwer Academic Publishers*

## 1. Introduction

Certain organic acid vapours are known to corrode metals like copper, steel, nickel, zinc, aluminium and magnesium in enclosed spaces (packages or containers) during storage and transportation [1–6].

Organic acid anions constitute about 0.1 to 1% of the total ion concentration in the corrosion-products (patina) on copper exposed to outdoor atmospheres for long periods [6]. The presence of formic and acetic acids has been also detected in rainwater [7, 8].

In the case of packaged parts and machinery, acetic acid vapour is released by woods and certain paints, plastics, rubbers, resins and other materials likely to be found alongside packaged metal items. This is especially the case in tropical conditions, due to the high temperatures, humidity and attack by micro-organisms, as well as the hydrolysis of the polyvinyl acetate used as binder [9–11]. Acetic acid vapours are also present in industrial atmospheres, e.g. from vinegar in the food processing industry and from the decomposition of raw materials in the paper industry.

Other acids can also cause copper deterioration. Thus, wood, plywood and chipboard binding resins and some rubbers and paints give off highly corrosive formic acid vapours, mainly in hot humid environments [12]. In automobiles, the high temperature decomposition of ethylene glycol produces formic acid. The hydrolysis of chlorinated organic solvents also produces carboxylic acids [13].

Formic, acetic and propionic acids have been associated with early corrosion failure of copper tubes used in air-conditioning and heat exchanger systems, which has been described in the literature as "ant-nest" corrosion [9, 13–17]. Both formic and acetic acids cause metal corrosion at very low concentrations [6, 7, 13].

The aim of this paper is to study the corrosion behaviour of copper exposed to formic and acetic acid vapours for a short period of time (21 days) at 100% relative humidity. The solid phases formed on copper surfaces were analysed in order to contribute to knowledge of the effect of these vapours on the atmospheric corrosion mechanism of copper.

## 2. Materials and methods

The experimental procedure has been described elsewhere [18, 19]. Corrosive environments were generated in an airtight 2.4 l glass vessel. In order to obtain a vapour concentration of formic or acetic acid, it was assumed that the partial pressure of solvent vapour in equilibrium with a dilute solution is directly proportional to the mole fraction of solvent in the solution,

$$P = \chi P_0 \tag{1}$$

which is the expression of Raoult's law [18], where $P$ is the partial pressure of the solvent (formic or acetic acid) above the solution (in mm Hg), $P_0$ is the vapour pressure of the pure solvent (formic or acetic acid), and $\chi$ is the mole fraction of solvent in the mixed aqueous solution (pure formic or acetic acid and distilled water).

The concentration of formic or acetic acid in the vapour phase ($C$), expressed in ppm (parts per million, $10^6$, by weight), can be written as

$$C = \frac{\left(\frac{P}{760}\right)M}{29} 10^6 = 45.37\,\mathrm{MP} \tag{2}$$

where $M$ is the molecular weight of formic or acetic acid, 760 is the amount of mm Hg in one atmosphere, and 29 is the molecular weight of air.

If $G$ is the mass of formic or acetic acid, expressed as number of grammes in a 1000 ml solution, then $\chi$ can be written as

$$\chi \approx \frac{G/M}{1000/18} = 1.8 \times 10^{-2}\mathrm{G/M} \quad (3)$$

where 18 is the molecular weight of water.

Taking into account Equations 1, 2 and 3, it is possible to write

$$\frac{C}{45.37M} = 1.8 \times 10^{-2}(G/M)P_0 \quad (4)$$

therefore

$$G = 1.22\frac{C}{P_0} \quad (5)$$

The $P_o$ value was obtained from Fig. 1. This was drawn using data from the literature and the Claussius-Clapeyron equation ($\log P_0 = -A/T + B$) [20]. It can be observed that for both acids the log $P_o$ value decreases as $1/T$ increases and that for a given temperature, $P_o$ is higher for formic acid than for acetic acid.

The relative humidity (RH) of approximately 100% was obtained by placing 350 ml of distilled water in the bottom of the airtight glass vessel, with the copper specimens placed on a perforated ceramic grill situated above the distilled water.

Five formic and acetic acid concentrations: 10, 50, 100, 200 and 300 ppm were tested. The vapour concentration of formic or acetic acid was obtained by replacing the 350 ml of distilled water at the bottom of the airtight glass vessel with a solution containing the appropriate amount of 85% formic acid (Merck) or glacial acetic acid (Merck), in line with Equation 5. These acid levels were chosen in order to accelerate the copper corrosion process in the laboratory, with the aim of following the evolution process of the patina from its origin stage up to 21 days experimentation.

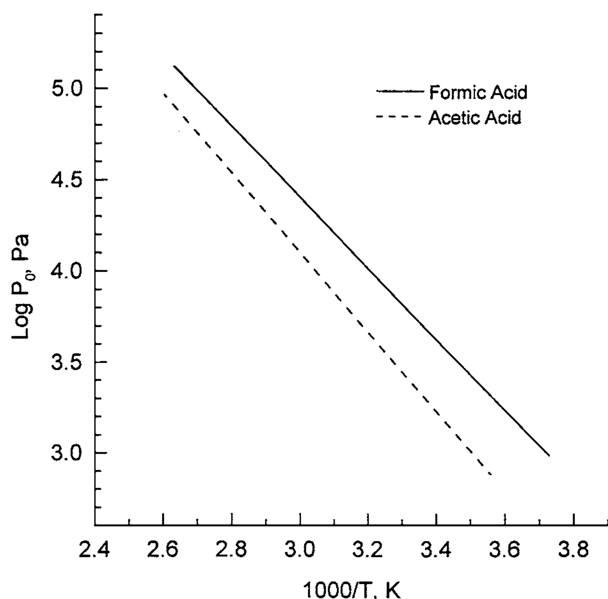


*Figure 1* Vapour pressure (in pascal, Pa) against Kelvin temperature of formic and acetic acids.

The copper used had the following chemical composition (mass %): 0.015 Pb, 0.009 Sn, <0.001 Al, <0.002 Sb, <0.001 As, <0.001 Bi, <0.001 Fe, 0.003 Ni, 0.019 P, <0.001 Mn, with the balance in Cu. The copper was phosphorus-deoxidised and had a low residual phosphorus content (type Cu-DLP, ISO 1337 Standard). Mechanically polished specimens were prepared with different grades of emery paper in dry conditions down to grade 600 and tested immediately.

Vertically suspended 5 cm × 5 cm copper specimens were exposed to the action of formic or acetic acid vapour for a period of 21 days. The temperature was held at 30°C during the experiments by immersing the airtight glass vessel in a thermostatically controlled water bath. At the end of these experiments the nature of the surface corrosion products was determined. For comparative purposes a copper reference specimen was exposed to an uncontaminated 100% RH atmosphere under identical experimental conditions.

Gravimetric tests were carried out taking measurements at the beginning of the experiments and at their end, following the removal of the corrosion products using a 10% $H_2SO_4$ aqueous solution, in accordance with ASTM G-1 Standard. The experiments were performed in triplicate, i.e. the gravimetric corrosion rate is listed as the average value of three specimens studied under identical experimental conditions. The reproducibility of the gravimetric experimental results was higher than 95%. An electronic analytical balance with a precision of ±0.1 mg was utilised.

Electrochemical studies were performed by cathodic reduction using a EG&G PARC, model 273A, potentiostat/galvanostat. The classic three-electrode configuration was utilised, employing a saturated calomel electrode (SCE) as reference and a platinum gauze cylinder of 36 cm$^2$ area as the counter electrode. The surface of the specimen was masked using a corrosion protection tape, leaving an uncovered area of 1 cm$^2$ as the working electrode. Experiments were carried out under static conditions at room temperature. A 0.1 M sodium borate solution (500 ml) pH $\sim$ 9 and analytical-grade was utilised as supporting electrolyte for the cathodic reduction experiments [21]. The solution was de-aerated by bubbling nitrogen through the system for one hour before the start of experimentation and throughout its duration.

The solid phases formed on the copper surface were characterised by X-ray powder diffraction (XRD), employing a Siemens D-500 diffractometer with monochromatised Cu K$\alpha$ radiation. Patterns were recorded from 10 to 60 2$\theta$ degrees, in the step scanning mode, with a 0.025° (2$\theta$) step and 2 s counting time.

A Jeol JXA-840 scanning electron microscope (SEM) was utilised to perform morphological observations. Conducting specimens for SEM were prepared by gold sputtering the copper specimens.

## 3. Results and discussion

Fig. 2 reports the corrosion rate estimated from gravimetric data, expressed as milligram per metre$^2$ per day (mmd), for copper exposed to formic and acetic acid vapours for 21 days experimentation. It can be observed

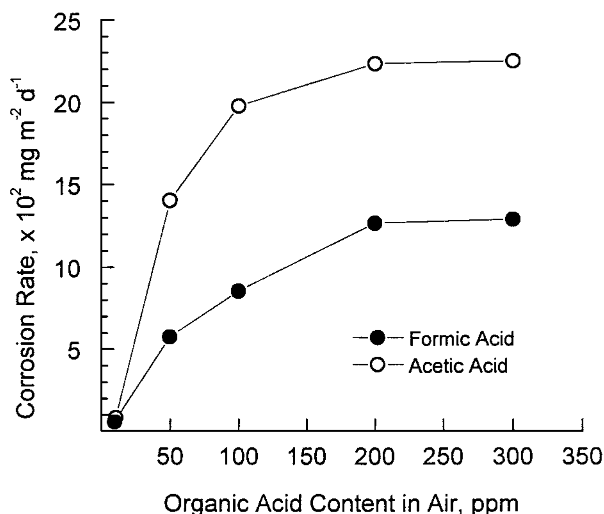


*Figure 2* Copper corrosion rate against formic and acetic acids content in the atmosphere of an airtight 2.4 l glass vessel, after 21 days' exposure at 100% RH and 30°C. Corrosion rate was expressed as milligram per metre$^2$ day (mmd).

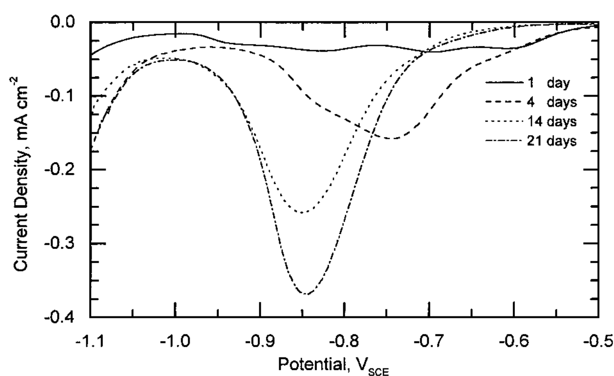


*Figure 3* Reduction scans in a 0.1 M de-aerated sodium borate solution for copper exposed to 10 ppm of formic acid vapour. The scans were obtained at a potential sweep rate of 1 mV s$^{-1}$ starting at the open circuit potential.

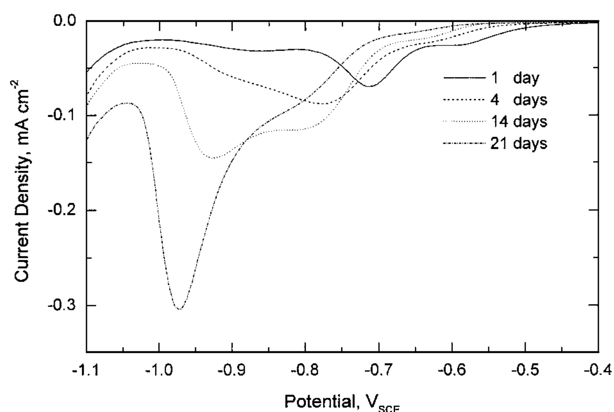


*Figure 4* Reduction scans in a 0.1 M de-aerated sodium borate solution for copper exposed to 10 ppm of acetic acid vapour. The scans were obtained at a potential sweep rate of 1 mV s$^{-1}$ starting at the open circuit potential.

that the copper corrosion rate increases in line with the increase in both formic and acetic concentrations. The copper corrosion rate increases following the parabolic law of formic and acetic acid vapour concentration dependence. This behaviour is typical of materials where the corrosion product layer plays an important role in the protection of the material [1]. There seems to be a formic and acetic acid vapour contamination threshold (200 ppm) above which the corrosion rate stabilises. This may be related to the formation of a copper compound which protects the copper surface. Formic acid vapour gave a lower copper corrosion rate than acetic acid vapour. For instance, at 300 ppm formic acid vapour caused a copper corrosion rate of 1300 mmd, while acetic acid vapour gave 2300 mmd.

Considering that the dissociation constant in aqueous solution is higher for formic acid than for acetic acid ($1.77 \times 10^{-4}$ and $1.76 \times 10^{-5}$ at 25°C, respectively), formic acid vapour may be expected to originate a higher copper corrosion rate than acetic acid vapour [22]. The nature of the corrosion products is influenced by the corrosivity of the vapour phase formic or acetic acid. In the presence of formic acid vapour the corrosion product layer was very compact and adherent, while in the presence of acetic acid vapour it was poorly adherent and of a porous nature. This may explain why formic acid vapour gave a lower corrosion rate than acetic acid vapour. These results agree with the literature for the case of mild steel vapour phase corrosion [1, 12].

Fig. 3 shows cathodic reduction curves for copper specimens exposed to 10 ppm of formic acid vapour for several exposure times. Four peaks can be observed in the plot corresponding to one day of experimentation. The first peak, located at $-0.6$ $V_{SCE}$, has been attributed to the reduction of amorphous cuprous oxide (cuprite, $Cu_2O$). The second peak, at $-0.69$ $V_{SCE}$, is attributed to the reduction of copper (II) hydroxide monohydrate ($Cu(OH)_2 \cdot H_2O$) [23, 24]. The third peak, at $-0.83$ $V_{SCE}$, is attributed to the reduction of amorphous copper formate grown on the initial amorphous cuprite [23–27]. Finally, the fourth peak, observed at approximately $-0.92$ $V_{SCE}$, should be attributed to copper formate. Similar information was obtained for 4, 14 and 21 days experimentation.

Fig. 4 shows cathodic reduction curves for copper specimens exposed to 10 ppm of acetic acid vapour. Three peaks can be observed in the plot corresponding to one day experimentation. The first peak, located at $-0.6$ $V_{SCE}$, has been attributed to the reduction of amorphous cuprite [23, 24, 28, 29]. This $Cu_2O$ layer is frequently formed by copper exposure to uncontaminated air. The second peak, at $-0.71$ $V_{SCE}$, is attributed to the reduction of crystalline cuprite formed on the initial amorphous cuprite. Finally, the third peak, observed at approximately $-0.9$ $V_{SCE}$, should be attributed to copper acetate, as is explained later in the text. As in Fig. 3, similar information was obtained for 4, 14 and 21 days.

In general, formic and acetic acid vapours at 10, 100 and 300 ppm show a potential peak shift to more cathodic values with experimental time as the formic and acetic acid vapour contents in the air increase. This behaviour may be associated with the thickening of the patina layer. One of the most important differences between formic and acetic acid vapours is that copper hydroxide is formed only in the presence of formic acid.

Fig. 5 shows the recorded potential against time plot for the cathodic stripping of copper exposed to 10 ppm

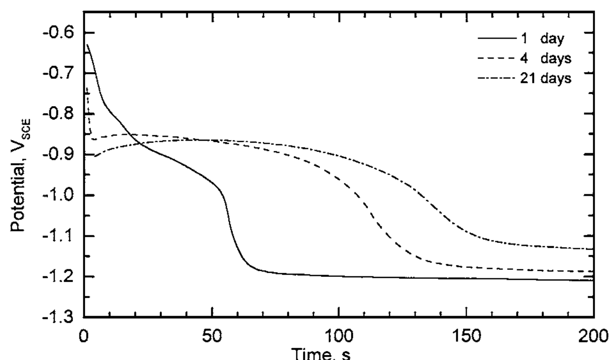


*Figure 5* Cathodic stripping for copper exposed to 10 ppm of formic acid vapour. A 0.1 M de-aerated sodium borate solution was used as supporting electrolyte. Current density 250 $\mu$A cm$^{-2}$.

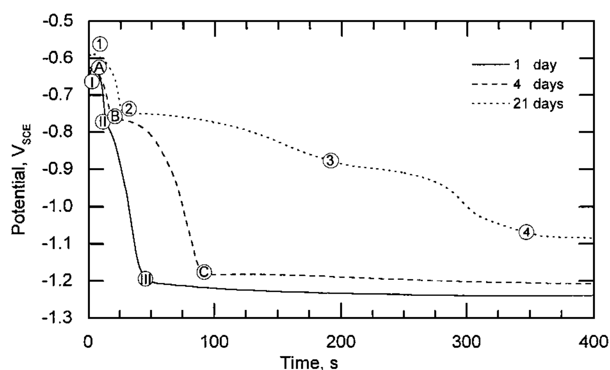


*Figure 6* Cathodic stripping for copper exposed to 10 ppm of acetic acid vapour. A 0.1 M de-aerated sodium borate solution was used as supporting electrolyte. Current density 250 $\mu$A cm$^{-2}$.

of formic acid vapour using a 0.1 M de-aerated sodium borate solution. Two reduction regions can be observed at −0.77 $V_{SCE}$ and −0.87 $V_{SCE}$ in the plot corresponding to one day experimentation. In the plots for 4 and 21 days a broad plateau can be observed between −0.82 and −0.88 $V_{SCE}$, after which the appearance of hydrogen bubbles on the copper surface caused the potential to stabilise, indicating that all the corrosion products on the copper had been reduced and that the copper surface was being cleaned.

Fig. 6 shows cathodic stripping curves for copper specimens exposed to 10 ppm of acetic acid vapour. Two and three reduction regions can be observed. Regions I-II and II-III for one day, A-B and B-C for 4 days and 1-2 for 21 days were defined by a drop in potential followed by a small plateau, in turn followed by an inflection point. An extensive plateau, regions 2-3 and 3-4 for 21 days, was formed before the second and third inflection points, after which the potential stabilised.

The layer thickness was determined using Faraday's law [30, 31]. The transition from one reduction process to the next has been determined by a peak in the first derivative of the experimental data, in accordance with ASTM B-825 Standard. Thickness data was calculated assuming the average density of oxide layers in the region of −0.77 $V_{SCE}$ to be equal to that of copper (II) hydroxide monohydrate (3.37 g cm$^{-3}$), those in the region from −0.82 to −0.88 $V_{SCE}$ to be equal to that of copper formate (1.81 g cm$^{-3}$), those in regions 1-2, A-B, and I-II to be equal to that of amorphous cuprite (6.0 g cm$^{-3}$), and those in region 2-3, B-C, and II-III equal to that of cuprite (6.0 g cm$^{-3}$). Finally, region 3-4 was attributed to copper acetate (1.88 g cm$^{-3}$). Despite a lack of information about the surface roughness factor of the specimens, and assuming the layer to be uniform, the thickness under conditions appertaining to Figs 5 and 6 was approximately as indicated in Table I. As can be observed, the corrosion product layer is thicker for formic acid than for acetic acid.

TABLE I Thickness of corrosion-product layer for copper exposed to 10 ppm formic and acetic acid vapours

| Acid | Time (days) | Compound | Thickness (nm) |
|---|---|---|---|
| Formic | 1 | Amorphous cuprite | 2.78 |
| | | Cupric hydroxide | 5.62 |
| | | Copper formate | 72.66 |
| | 4 | Copper formate | 213.13 |
| | 11 | Copper formate | 250.26 |
| | 21 | Copper formate | 264.79 |
| Acetic | 1 | Amorphous cuprite | 4.0 |
| | | Cuprite | 11.1 |
| | 4 | Amorphous cuprite | 5.9 |
| | | Cuprite | 22.6 |
| | 11 | Amorphous cuprite | 8.7 |
| | | Cuprite | 48.8 |
| | 21 | Copper acetate | 225.4 |

Fig. 7 depicts XRD patterns recorded from 10 to 60 2$\theta$ degrees for all the specimens exposed to formic acid

*Figure 7* XRD patterns for copper exposed to 0, 10, 50, 100, 200 and 300 ppm of formic acid for a period of 21 days, Cu = metallic copper, c = cuprite, x = copper hydroxide monohydrate and f = copper formate.

vapour. The diagrams corresponding to specimens exposed to an uncontaminated atmosphere (0 ppm) and 10 ppm of formic acid vapours were obtained from direct analysis of the specimens. Patterns for the other specimens were recorded from analysis of the powdered solids from scratched specimens. In Fig. 7 the XRD pattern for the specimen exposed to an uncontaminated atmosphere (pattern labelled 0) only shows the reflections $d_{111}$ ($2\theta = 43.32°$) and $d_{200}$ ($2\theta = 50.47°$) corresponding to metallic copper. For specimens exposed to 10 ppm of formic acid vapour, the XRD pattern, in addition to metallic copper peaks, shows maximums for the reflections $d_{001}$ ($2\theta = 13.25°$) and $d_{002}$ ($2\theta = 26.72°$) corresponding to copper (II) hydroxide monohydrate [JCPDS 42-746] (peaks labelled x). The XRD patterns for copper specimens exposed to 50 and 100 ppm of formic acid vapour show the presence of $Cu(OH)_2 \cdot H_2O$ along with the diffraction maximums corresponding to cuprite [JCPDS 5-667] (peaks labelled c). As can be observed, a third not well-crystallised phase started to form at these contamination levels. This phase may consist of copper hydroxide formate (Cu(OH)(HCOO)), originated as an intermediate reaction product (see the reaction of Equation 12 later in the text). Peaks corresponding to cuprite decrease as the formic acid vapour level increases from 100 up to 300 ppm. A similar evolution is observed with copper hydroxide, in the pattern corresponding to specimens exposed to 300 ppm of formic acid vapour, in which diffraction maximums for that phase are hardly observed. Peaks corresponding to copper hydroxide formate start to appear in the pattern exposed to 200 ppm of formic acid vapour and are much better defined in the pattern corresponding to 300 ppm (peaks labelled f). Copper hydroxide formate may be assumed to be a tetrahydrate salt because of the first very strong reflection, $2\theta = 13.08°$, but the highly complex pattern may indicate a mix of different hydrate salts. Copper hydroxide formate seems to form from copper hydroxide, thus in the pattern corresponding to specimens exposed to 200 ppm of formic acid vapour both phases coexist, but as the concentration of formic acid in the vapour phase increases up to 300 ppm, peaks corresponding to copper hydroxide disappear. This may be explained by a dissolution-precipitation reaction mechanism.

Fig. 8 depicts XRD patterns for specimens exposed to 50, 100, 200 and 300 ppm of acetic acid vapour for 21 days exposure. The pattern for the specimens exposed to 10 ppm of acetic acid vapour is not included in the figure since it showed the peaks corresponding to metallic copper only, though the pattern background seems to indicate the presence of amorphous phases. The crystalline phases observed on the copper specimen exposed to 300 ppm of acetic acid vapour are copper acetate dihydrate ($Cu(CH_3COO)_2 \cdot 2H_2O$) [JCPDS 27-145], as the principal component, and cuprite [JCPDS 5-667]. The XRD patterns for 50 and 100 ppm of acetic acid vapours show the presence of a third phase, which may be attributed to copper hydroxide acetate dihydrate ($Cu_4(OH)(CH_3COO)_7 \cdot 2H_2O$) [18]. This phase (peaks labelled h) starts to form on the 50 ppm of acetic contamination specimen, is the principal component on the

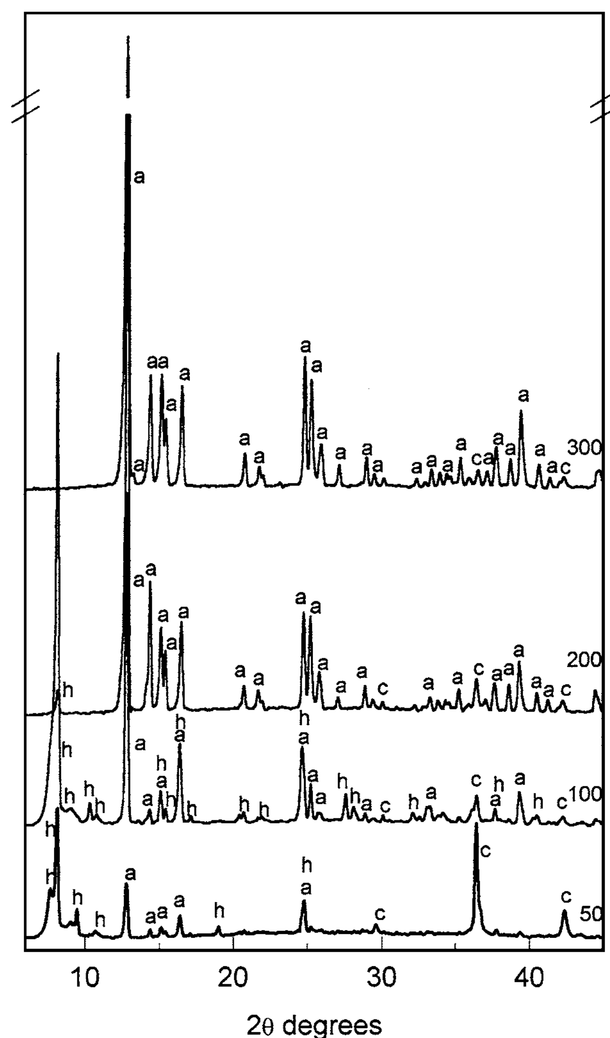


*Figure 8* XRD patterns for copper exposed to 50, 100, 200 and 300 ppm of acetic acid for a period of 21 days, c = cuprite, h = copper hydroxide acetate, and a = copper acetate dihydrate.

100 ppm acetic specimen, and is the minority component on the 200 ppm acetic specimen. In addition to copper hydroxide acetate dihydrate, all the XRD patterns show cuprite (peaks labelled c) and copper acetate dihydrate (peaks labelled a). The presence of basis copper acetate has been observed by the authors on patinas formed on copper exposed to laboratory and outdoor atmospheres [31]. According to XRD results the formation of copper hydroxide acetate dihydrate does not seem to take place from the cuprite layer. Depth-dependent XPS studies indicated a stratified structure from the metal interface to the atmosphere interface: $Cu_2O/CuO/Cu(OH)_2$ or $CuO \cdot xH_2O$ in the first passivating layer [26, 32, 33]. The presence of hydroxide or hydrated oxide at the initially exposed copper surface provides a building block for the formation of basis copper acetate. The formation of copper hydroxide acetate dihydrate may be as follows

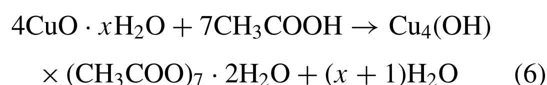

$$4CuO \cdot xH_2O + 7CH_3COOH \rightarrow Cu_4(OH) \times (CH_3COO)_7 \cdot 2H_2O + (x + 1)H_2O \quad (6)$$

This copper hydroxide acetate evolves to form copper acetate under the atmospheric conditions of high

concentration of acetic acid, by the reaction

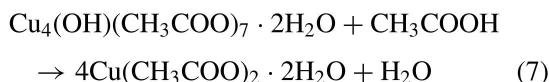

$$Cu_4(OH)(CH_3COO)_7 \cdot 2H_2O + CH_3COOH \rightarrow 4Cu(CH_3COO)_2 \cdot 2H_2O + H_2O \quad (7)$$

the final constituents of the patina being cuprite and copper acetate dihydrate. Thus, the presence of copper hydroxide acetate among the patina components could mean that the patination process has not yet finished.

According to XRD results, two main differences are observed on copper corrosion in the presence of formic and acetic acid vapours: (1) the formation of copper (II) hydroxide monohydrate even when the formic acid concentration is as low as 10 ppm. This compound was not observed as a crystalline phase in experiments conducted with acetic acid; and (2) the formation of copper formate salt at the expense of the copper hydroxide, which may indicate an acid-base reaction by means of a dissolution-precipitation mechanism. This salt started to form at concentrations above 100 ppm. In the case of acetic acid vapour, the formation of copper acetate or hydroxide (copper hydroxide acetate) starts at concentrations as low as 50 ppm. These salts seem to form by the reaction of acetic acid vapour with a depth layer of copper through porous cuprite paths.

In the first stage, when copper is exposed to 100% RH the water vapour that is adsorbed causes a corrosion process starting at local surface defects, and this process may be catalysed by formic acid. The first reaction taking place is

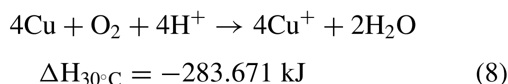

$$4Cu + O_2 + 4H^+ \rightarrow 4Cu^+ + 2H_2O \quad \Delta H_{30^\circ C} = -283.671\ \text{kJ} \quad (8)$$

and as the first solid corrosion product, whit formic acid, is copper hydroxide monohydrate ($Cu(OH)_2 \cdot H_2O$), accordingly the copper (I) must be oxidised

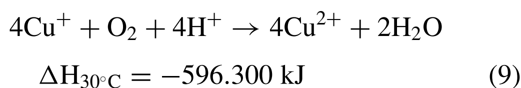

$$4Cu^+ + O_2 + 4H^+ \rightarrow 4Cu^{2+} + 2H_2O \quad \Delta H_{30^\circ C} = -596.300\ \text{kJ} \quad (9)$$

The reaction of Equation 9 is favoured in the case of formic acid due to the higher value of the dissociation constant as established above.

The cathodic reaction

$$O_2 + 2H_2O + 4e^- \rightarrow 4OH^- \quad \Delta H_{30^\circ C} = -270.908\ \text{kJ} \quad (10)$$

produces hydroxyl ions, which may migrate towards the anode to form copper hydroxide. The formation of copper hydroxide can take place during or after the dry-out of the droplets.

The presence of hydroxide or hydrated oxide on the initially exposed copper surface provides a building block for the formation of copper formate. The formation of copper formate may be as follows: (i) on local surface areas from $Cu(OH)_2 \cdot H_2O$

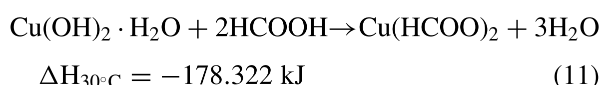

$$Cu(OH)_2 \cdot H_2O + 2HCOOH \rightarrow Cu(HCOO)_2 + 3H_2O \quad \Delta H_{30^\circ C} = -178.322\ \text{kJ} \quad (11)$$

However at a low formic acid concentration, the formation of copper hydroxide formates, as intermediate reaction products, may be considered according to the reaction

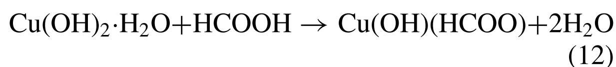

$$Cu(OH)_2 \cdot H_2O + HCOOH \rightarrow Cu(OH)(HCOO) + 2H_2O \quad (12)$$

(ii) Copper hydroxide formate spreads across the copper surface from cuprous ions. According to Notoya [13–15], a complex is formed between formic acid and cuprous ions, generated in the reaction of Equation 8

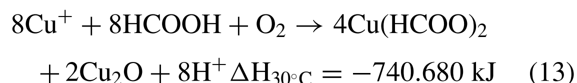

$$8Cu^+ + 8HCOOH + O_2 \rightarrow 4Cu(HCOO)_2 + 2Cu_2O + 8H^+ \Delta H_{30^\circ C} = -740.680\ \text{kJ} \quad (13)$$

In the reaction of Equation 13 both cuprite and cupric formate are formed. Cuprite can also be formed by

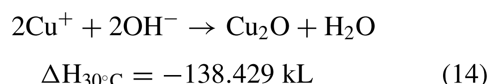

$$2Cu^+ + 2OH^- \rightarrow Cu_2O + H_2O \quad \Delta H_{30^\circ C} = -138.429\ \text{kL} \quad (14)$$

Hydroxyl ions are originated in the cathodic reaction, see the reaction of Equation 10.

Fig. 9 shows the SEM morphological aspect of an unexposed mechanically polished copper specimen included as a reference; in which the scratched surface can be observed. When copper is exposed to an uncontaminated 100% RH atmosphere for 21 days the corrosion process starts to occur as can be observed in Fig. 10. Corrosion starts in the deepest polished line, where water droplets are more easily retained.

Fig. 11 shows a SEM micrograph of a copper specimen exposed to 10 ppm of formic acid vapour for 21 days. It can be observed that the corrosion has spread further over the surface. The corrosion layer is non-uniform and corrosion products have grown on certain local surface areas from droplets of formic acid adsorbed on the surface. The acid molecules enter patination reactions by their incorporation in droplets, which subsequently interact with the copper to originate local attack. In these areas crystalline copper hydroxide has developed. Fig. 12 shows the general appearance of copper exposed to 50 ppm of formic acid vapour. It can be observed that the copper surface is totally covered with corrosion products. The corrosion layer thickness

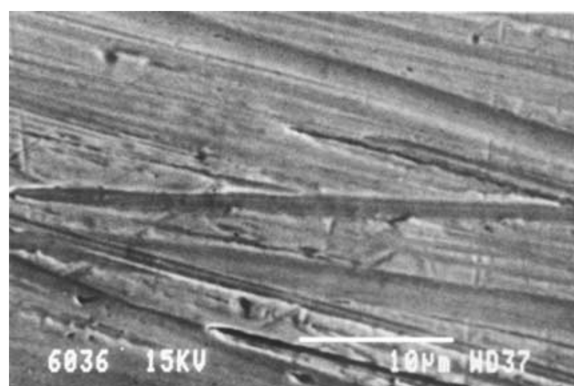


*Figure 9* SEM micrograph for an unexposed mechanically polished copper surface.

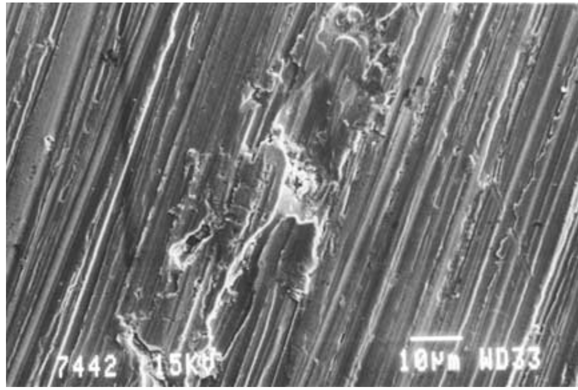


*Figure 10* SEM micrograph for a copper specimen exposed to an uncontaminated atmosphere at 100% RH for 21 days.

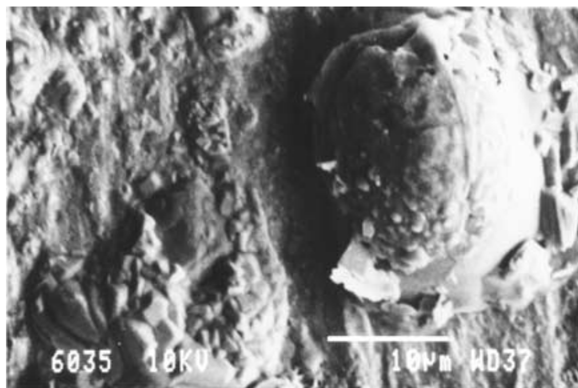


*Figure 11* SEM micrograph for a copper specimen exposed to 10 ppm of formic acid vapour for 21 days.

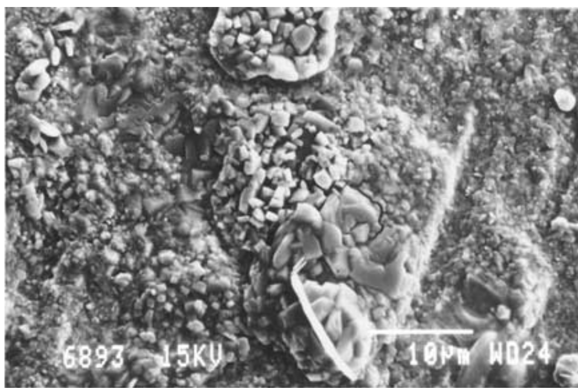


*Figure 12* SEM micrograph for a copper specimen exposed to 50 ppm of formic acid vapour for 21 days.

varies across the surface. It can also be observed that corrosion products have precipitated inside a ring from the deposition of a droplet. Fig. 13 shows different morphological aspects of corrosion products formed when copper is exposed to 100 ppm of formic acid vapour. At this level of formic acid vapour the corrosion layer is very porous and copper surface passiveness is not attained.

Fig. 14 shows a SEM micrograph of a copper specimen exposed to 10 ppm of acetic acid vapour for 21 days. It can be observed that the patination process follows the orientation of the polished surface. The non-homogeneous grain size of this first layer of copper (I) oxide is up to 1 $\mu$m. This phase is not crystallographically ordered and accordingly is amorphous to

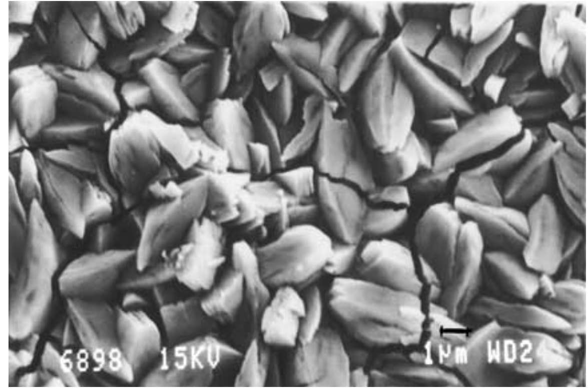


*Figure 13* SEM micrograph for a copper specimen exposed to 100 ppm of formic acid vapour for 21 days.

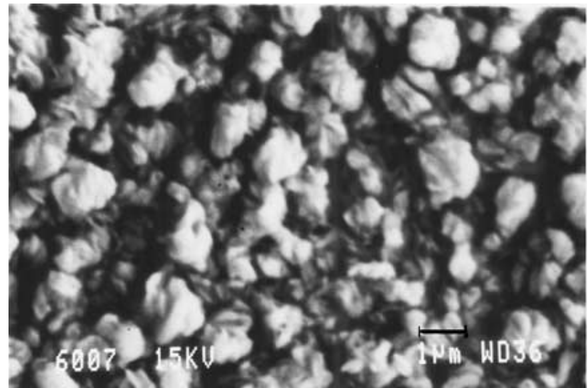


*Figure 14* SEM micrograph for a copper specimen exposed to 10 ppm of acetic acid vapour for 21 days.

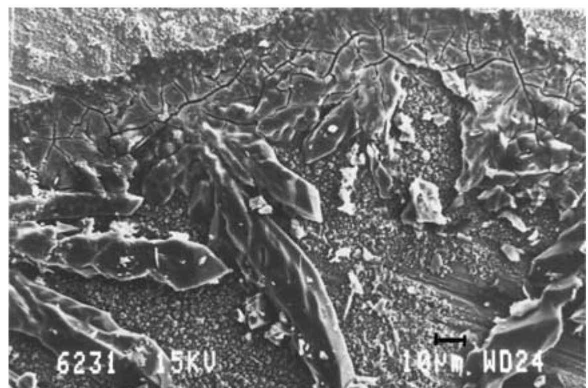


*Figure 15* SEM micrograph for a copper specimen exposed to 50 ppm of acetic acid vapour for 21 days.

the XRD. Fig. 15 shows a dark droplet, in which it is possible to see dendritic growth of copper hydroxide acetate from the droplet boundary, where the local concentration of acetic acid is higher, towards the interior of the droplet. The formation of copper hydroxide acetate does not seem to occur at the expense of the cuprite layer. Fig. 16 shows the general appearance of a copper surface exposed to 100 ppm of acetic acid vapour for 21 days exposure. It can be observed that the patina consists of irregular protuberances, such as hollow towers perpendicular to the copper surface. Some crystal macles of cuprite of 100 $\mu$m size can be observed.

Fig. 17 shows a SEM micrograph of a copper specimen exposed to 200 ppm of formic acid vapour for

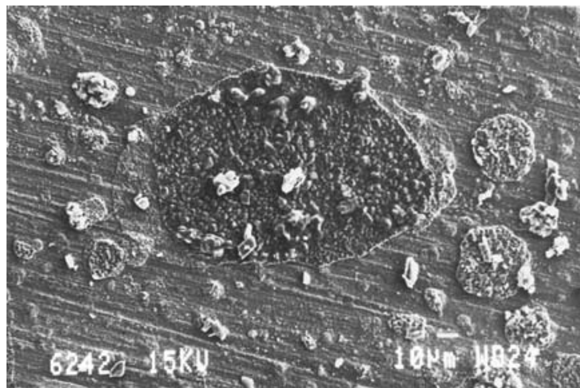


*Figure 16* SEM micrograph for a copper specimen exposed to 100 ppm of acetic acid vapour for 21 days.

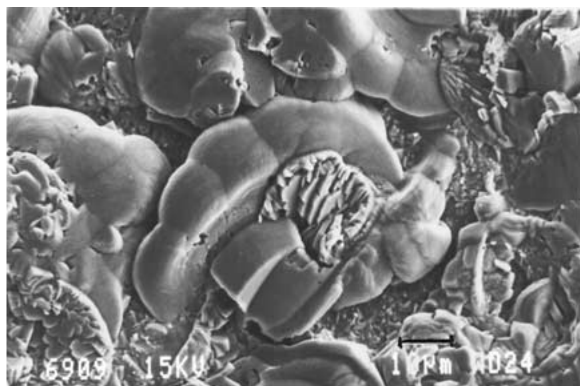


*Figure 17* SEM micrograph for a copper specimen exposed to 200 ppm of formic acid vapour for 21 days.

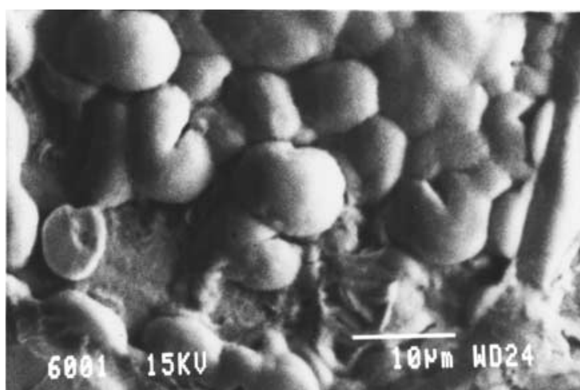


*Figure 18* SEM micrograph for a copper specimen exposed to 300 ppm of formic acid vapour for 21 days.

21 days. High crystalline growth can be observed with quite perfect crystals of copper hydroxide and cuprite. Copper formate seems to develop from later depositions. This morphology is consistent with a dissolution-precipitation mechanism for the formation reaction of copper formate. The wave-like and smooth-surface morphologies may indicate a rapid dry-out process. Fig. 18 shows a SEM micrograph of a copper specimen exposed to 300 ppm of formic acid vapour for 21 days. It can be observed that the copper surface is covered with a smooth-surface bubble-like layer.

Fig. 19 shows a SEM micrograph of a copper specimen exposed to 200 ppm of acetic acid vapour for 21 days exposure. It is possible to observe plate-like copper acetate crystals over the lower copper oxide phase. It should be pointed out that in this figure the cementation process of small oxide particles to the lower layer is yielded by the high concentrations of acetic acid. These results agree well with the mechanisms proposed by Graedel in relation with copper patina formation processes in atmospheres contaminated with organic compounds [34]. Fig. 20 shows a SEM micrograph of a copper specimen exposed to 300 ppm of acetic acid vapour for 21 days. Here the copper acetate layer covers all the copper surface, and not only local zones as in the previous specimen. In some zones it is possible to observe large size cuprite crystals which arise between the copper acetate crystals, showing an irregular growth pattern due to the high acetic acid vapour concentration.

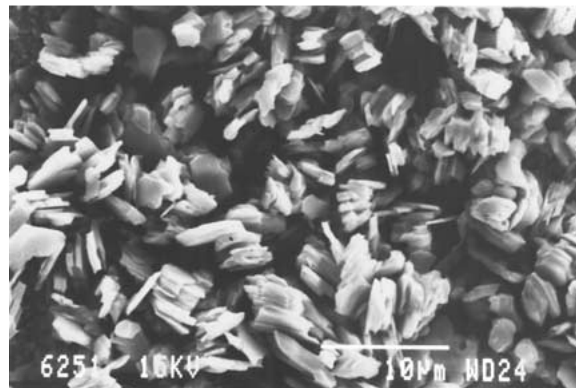


*Figure 19* SEM micrograph for a copper specimen exposed to 200 ppm of acetic acid vapour for 21 days.

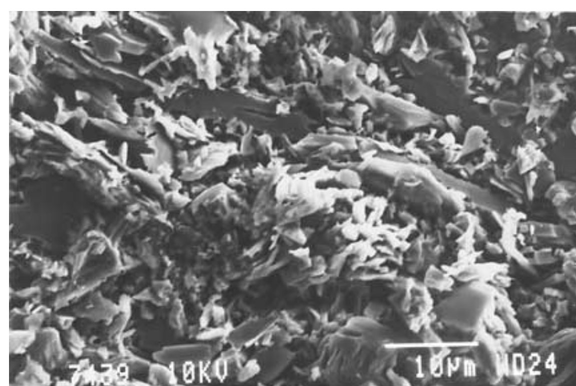


*Figure 20* SEM micrograph for a copper specimen exposed to 300 ppm of acetic acid vapour for 21 days.

## 4. Conclusions

Copper corrosion rate was in the range from 100 to 1300 mmd for the formic acid vapour and in the range from 100 to 2300 mmd for the acetic acid vapour, using 10, 50, 100, 200 and 300 ppm contamination levels for both acids at a 100% relative humidity for a period of 21 days exposure.

The main components of the patina were cuprite, cupric hydroxide monohydrate and copper formate tetrahydrate in the case of formic acid vapour. In the presence of acetic acid vapour, cuprite, copper acetate dihydrate and copper hydroxide acetate dihydrate were the main compounds identified. At low formic acid vapour concentrations, the components of

the patina were mainly cuprite and copper hydroxide. The latter formed during or after the dry-out of the adsorbed film of water and condensed formic acid vapour acid droplets on the copper surface. In the presence of low acetic acid vapour the molecules enter patination reactions by adsorption from the gas phase to the wetted copper surfaces. In both acid vapours the patina is initially developed in a uniform manner. At intermediate formic acid vapour concentrations a third not well-crystallised copper formate hydrate phase started to form. As the formic concentration increased from 100 up to 300 ppm, the cuprite and copper hydroxide components decreased and the presence of copper formate was more evident on local surface areas around droplets of formic acid adsorbed on the surface, originated by a dissolution-precipitation reaction mechanism. For the case of acetic acid vapour, as the acid concentration increases the copper hydroxide acetate and copper acetate start to develop on local zones from droplets of acetic acid adsorbed on the surface. This may indicate that at the highest acetic concentrations the reaction mechanism is different and in this case the molecules enter patination reactions by their incorporation in droplets, followed by the interaction of these droplets with the copper.

## Acknowledgement

The authors express their gratitude to the Regional Government of Madrid, Spain, for financial support under Project No. 07N/0043/1999.

## References

1. J. M. BASTIDAS and E. M. MORA, *Can. Metall. Quart.* **37** (1998) 57.
2. P. D. DONOVAN and J. STRINGER, *Brit. Corros. J.* **6** (1971) 132.
3. G. REINHARD and C. IRMSCHER, *Werkst. Korros.* **32** (1981) 377.
4. D. CERMÁKOVÁ and Y. VLCHKOVA, in Proc. 3rd Inter. Congr. Metallic Corros., Moscow, 1966, p. 497.
5. S. G. CLARKE and E. E. LONGHURST, *J. Appl. Chem.* **11** (1961) 435.
6. T. E. GRAEDEL, C. MCCRORY-JOY and J. P. FRANEY, *J. Electrochem. Soc.* **133** (1986) 452.
7. J. N. GALLOWAY and G. E. LIKENS, *Water Air Soil Poll.* **6** (1976) 241.
8. W. C. KEENE, J. N. GALLOWAY and J. D. HOLDEN, JR., *J. Geophys. Res.* **88** (1983) 5122.
9. J. O. EDWARDS, R. I. HAMILTON and J. B. GILMOUR, *Mater. Performance* **16** (1977) 18.
10. A. R. PARKINSON, *Anti-Corros.* **37** (1990) 11.
11. P. D. DONOVAN, in "Protection of Metals From Corrosion in Storage and Transit" (Ellis Horwood, a division of John Wiley, Chichester, England, 1986) p. 78.
12. D. KNOTKOVÁ-CERMÁKOVÁ and Y. VLCHKOVA, *Brit. Corros. J.* **6** (1971) 17.
13. T. NOTOYA, *J. Mater. Sci. Lett.* **10** (1991) 389.
14. *Idem.*, *ibid.* **16** (1997) 1406.
15. *Idem.*, *Mater. Performance* **32** (1993) 53.
16. E, CANO, J. SIMANCAS, J. L. POLO, C. L. TORRES, J. M. BASTIDAS and J. ALCOLEA, *Mater. Corros.* **50** (1999) 103.
17. J. M. BASTIDAS, M. P. ALONSO, E. M. MORA and B. CHICO, *ibid.* **46** (1995) 515.
18. A. LOPEZ-DELGADO, E. CANO, J. M. BASTIDAS and F. A. LOPEZ, *J. Electrochem. Soc.* **145** (1998) 4140.
19. J. M. BASTIDAS, A. LOPEZ-DELGADO, E. CANO, J. L. POLO and F. A. LOPEZ, *ibid.* **147** (2000) 999.
20. D. R. LIDE (ed.), "CRC Handbook of Chemistry and Physics," 71st ed. (CRC Press, Boca Raton, FL, 1990) p. 6.54.
21. E. M. M. SUTTER, C. FIAUD and D. LINCOT, *Electrochim. Acta* **38** (1993) 1471.
22. D. R. LIDE (ed.), "CRC Handbook of Chemistry and Physics," 71st ed. (CRC Press, Boca Raton, FL, 1990) p. 8.35.
23. M. LENGLET, K. KARTOUNI and D. DELAHAYE, *J. Appl. Electrochem.* **21** (1991) 697.
24. R. L. DEUTSCHER and D. WOODS, *ibid.* **16** (1986) 413.
25. R. E. V. D. LEEST, *Werkst. Korros.* **37** (1986) 629.
26. Y.-Y. SU and M. MAREK, *J. Electrochem. Soc.* **141** (1994) 940.
27. Y. FENG, W.-K. TEO, K.-S. SIOW, Z. GAO, K.-L. TAN and A.-K. HSIEH, *ibid.* **144** (1997) 55.
28. C. FIAUD, M. SAFAVI and J. VEDEL, *Werkst. Korros.* **35** (1984) 361.
29. B. I. RICKETT and J. H. PAYER, *J. Eletrochem. Soc.* **142** (1995) 3713.
30. J. M. BASTIDAS, A. LOPEZ-DELGADO, F. A. LOPEZ and M. P. ALONSO, *J. Mater. Sci.* **32** (1997) 129.
31. A. LOPEZ-DELGADO, J. M. BASTIDAS, M. P. ALONSO and F. A. LOPEZ, *J. Mater. Sci. Lett.* **16** (1997) 776.
32. H.-H. STREHBLOW and B. TITZE, *Electrochim. Acta* **25** (1980) 839.
33. E. OTERO, J. M. BASTIDAS, W. LOPEZ and J. L. G. FIERRO, *Werkst. Korros.* **45** (1994) 387.
34. T. E. GRAEDEL, *Corros. Sci.* **27** (1987) 721.

*Received 21 September 2000*
*and accepted 25 July 2001*